ISSN 2229-5518

Power Factor Control Using Auto Tuning Regulator

Gordon Ononiwu, Justine Onwumere, James Onojo, Longinus Ezema

Abstract- This paper presents the design of an auto tuning regulator that enhances the performance of the Static Var Compensator (SVC) technique. The Control law presented in this paper is based on the difference between a set point and measured system parameters. The scheme works on real time measurements from Instrument transformers, obtained from samples taken every 0.1s. Embedded Algorithms enable the control system to calculate and display relevant information through a display. Since the demand and supply of reactive power affects the power factor, instantaneous values of operating parameters are calculated through the embedded algorithms. The desired power factor is set and the controller determines the corresponding Vars. The controller constantly compares the set and measured values. With deviation, the controller tunes automatically to determine the new controller gains required to balance the disturbance. The SVC technique was used because it serves best when reactive power supply is to be localized at the point of demand. Models for SVC, Proportional-Integral – Derivative (PID), and the control module were derived from which the overall system transfer function was obtained. Simulation was carried out to validate the operation of the controller using a Matlab tool. A response of 0.199s rise time, 2.20s settling time, 2.64% overshoot shows an improved performance.

Index Terms - SVC, Regulator, PID, Power factor, Compensation, Control, Auto tuning, Reactive Power

1 Introduction

THE use of Static Var Compensation (SVC) for power factor correction and voltage stability has been an age long practice. Here, a controller is introduced to further enhance the efficiency and performance of the SVC technique. Various controllers have been implemented using FACTS devices for power factor improvement on distribution system [1]. The adaptive controller offers a solution to the difficulty experienced in tuning controllers when non linear loads are connected across the load bus [2]. This is easily tuned and the steady state error is reduced to a barest minimum [3].

The architecture of the controller involves measurement units, calculation unit, configuration unit, comparator, PID controller, Firing pulse generator and power unit. All these are required for the controller to monitor the network, determine network parameters and operating conditions, detect changes in network parameters, tunes automatically to promptly normalize the network in terms of voltage stability and power factor correction [4]. The controller receives network data in real time while the system is operating and functions based on Parameter Adaptation (PA). Parameters in this context refer to observable and controllable set of elements - the state variables. Adaptive technology is used because the power system dynamics are constantly changing and all the disturbance the network might experience are not known in advance [5]. Conventional controllers with fixed parameters are not able to adjust to network changes experienced during operation. Adaptive controller estimates uncertain network parameters on-line (real power, reactive power, power factor etc) while using measured system signals (voltage and current) [6].

1.1 Method of Adaptation

In [7], detail explanations were provided on various ways in which a controller can adapt to process dynamics. This ways includes: Gain Scheduling (GS), Model Reference Adaptive Control (MRAC) and Self-tuning Adaptive Control (SAC). Fig. 1 shows the block diagram of self tuning adaptive control module.

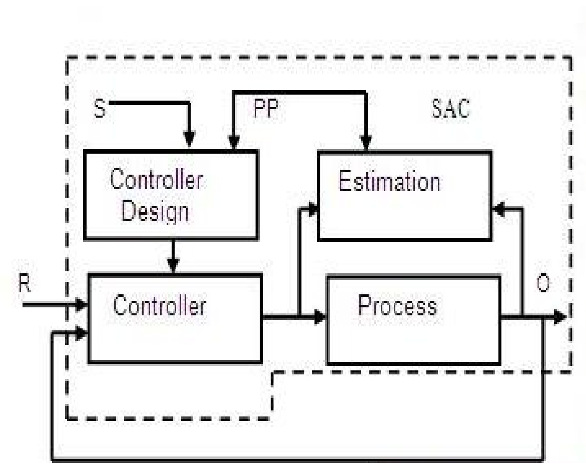

Fig. 1. Block Diagram of Self-tuning Adaptive Control (SAC) [1]

Where: S- Specifications
CP- Controller Parameters
PP- Process Parameters
R- Reference Input
O- Output

This paper proposes a Parametric Adaptive control based on Self tuning Regulator to monitor and maintain power factor as close as possible to unity. Due to the importance of power factor, several methods have been used in its control [8] which includes:

- Static capacitors
- Synchronous condensers
- Phase Advancers

The above methods are able to provide partial, fixed or over compensation due to their inability to adapt to the power system dynamics [9]. For optimal compensation, an adaptive controller is most recommended.

Adaptive approach is used due to the fact that power system parameters are always changing and uncertain, making other methods of control difficult to use. The adaptive power factor controller is a self-tuning controller, which provides real time monitoring and control based on acquired system parameters. In this approach, the power factor is controlled in a closed loop and the network parameters are obtained on-line using sensors (instrument transformer and current transformers) while the power system is operating. The controller is set to refresh at intervals for continuous monitoring and data acquisition, accurate inventions are made in the control loop to fulfill the desired power factor.

2 REVIEW OF RELATED WORKS

The use of filters to reduce harmonic distortion allowing only waveforms with frequency 50/60Hz to pass through the system was proposed in [10]. The idea is to linearize non –linear loads as the harmonic currents are filtered out. The simulation showed a reduction of harmonic distortion. By reducing the apparent power drawn from the ac supply, they achieved better power quality and minimized the power losses but were not able to make the load circuitry entirely resistive and linear. The amount of compensation required also poses a problem to rating of the filter. The higher the compensation required, the higher the value of the high-current inductors needed which are bulky and expensive.

In [11], Pulse Width Modulated Voltage Source Inverter (PWM-VSI) for power factor correction was proposed. It operates with fixed switching frequency providing compensation for reactive power and the harmonic current of non-linear loads. The active filter, DC capacitor cancels the initial distortion caused by the non –linear loads by injecting equal and opposite current harmonic components at the point of connection. Thereby improve the power factor of the power system. It functions on a simplified circuitry but reactive power compensation is done without sensing and computation of required data which poses a compromise on accuracy of compensation.

The laboratory prototype of power factor correction circuit was designed and implemented on a brushless DC motor control in [12]. Two PI controllers were used- one for the current control loop and the other for the voltage control loop. The results present a workable and cost effective power correction scheme for a Brushless DC Motor but yet to be implemented on the distribution network.

3 METHODOLOGY

A. Design Objective

The aim of this design paper is to optimize the power factor control using PID design technique. The major objective is to design a controller that will adapt to power system dynamics and improve the performance of Static Var Compensation method. The controller is targeted to provide fast response to commands with minimized overshoots and oscillations, return and maintain the power factor to desired value after a disturbance. The system architecture is presented in Fig. 2.

B. Design Specification

The controller design specifications aimed at in this design using MATLAB tool are as follows:

- Overshoot less than 5%
- Rise time less than 3 seconds
- Settling time less than 3 seconds

C. Design Architecture

The load bus is monitored through current and voltage signals from the Instrument Transformers which is referred to as the measuring module. These signals are displayed to the operator through the Human Machine Interface (HMI). Real Power, Reactive Power, Power factor, Total Harmonic Distortion are determined from these signals through embedded algorithm. The control Law is to determine the error between the set power factor and system operating power factor. This error is fed into the PID controller which tunes automatically to determine the required pulses and compensation to stabilize the system. The compensation is divided into stages.

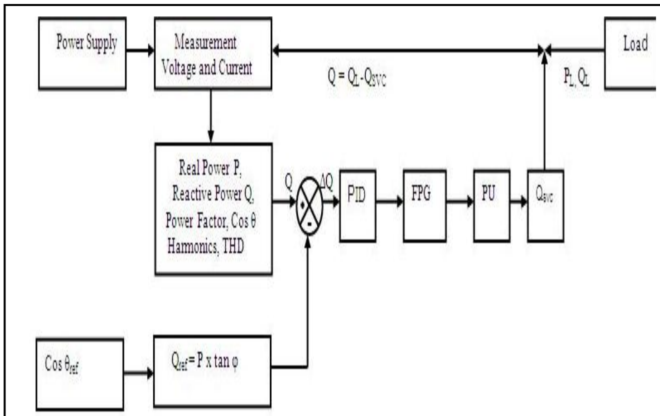

Fig. 2. Architecture of Adaptive Control System
Cosθref – reference power factor, α – Thyristor firing angle, FPG- Firing pulse generator, PU – Power Unit, Qref- Reference reactive Power

ISSN 2229-5518

3.1 Mathematical Models

A. Modeling of SVC

This paper presents a Thyristor Control Reactor (TCR) and Fixed Capacitor (FC) model of SVC. There are several models of SVC [13], TRC/FC models is used because this model function better where reactive power generation and absorption is required ([13].

This enables the reactor to function as a controllable susceptance, in the inductive sense, which is a function of the firing angle α [14].

Case 1: Full conduction, $\alpha = \frac{\pi}{2}$

When no harmonics is generated into the circuit, $\alpha = \frac{\pi}{2}$

The thyristors are gated into account and the reactors are fully conducting. Then current flowing through the reactor at this point is sinusoidal and lags the voltage by almost 90° (π/2). This condition corresponds to a firing angle of π/2 which is the current zero-crossing measured with reference to the voltage zero-crossing [14].

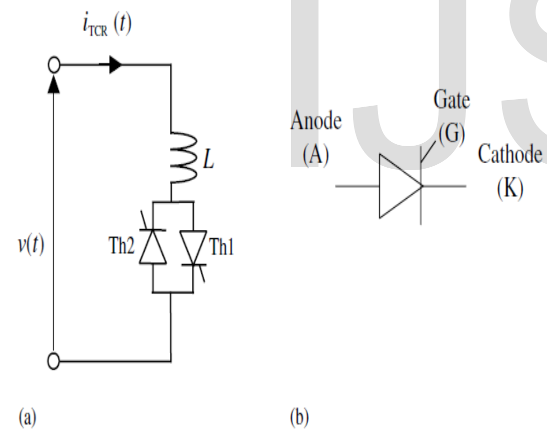

Fig. 3. (a) Basic thyristor-controlled reactor (TCR); (b) thyristor circuit symbol [13].

$$\sigma = 2(\pi - \alpha) \qquad (1)$$

Where σ– conduction angle of the thyristor, α – firing angle of the thyristor

Case 2: Partial conduction, $\frac{\pi}{2} < \alpha < \pi$ (1a)

When the firing angle is increased above π/2, the TCR current waveform becomes non sinusoidal thereby introducing harmonics into the system [15].

$$i_{TCR} = \frac{1}{L}\int_{\sigma}^{\omega t} v(t)dt, \text{ But } v(t) = \sqrt{2V}\sin\omega t \qquad (1b)$$

$$i_{TCR} = \frac{\sqrt{2V}}{\omega L}(\cos\sigma - \cos\omega t) \qquad (2)$$

2

For $\alpha \le \omega t \le (\alpha + \sigma) else 0$

The fundamental current is derived using Fourier analysis,

$$I_{TCRf1} = \frac{V}{J\pi\omega L}[2(\pi - \sigma) + Sin2\alpha] \qquad (3)$$

$$I_{TCRh} = \frac{4V}{j\omega L}\left|\frac{\sin(h+1)\alpha}{2(h+1)} + \frac{\sin(h-1)\alpha}{2(h-1)}\cos\alpha(\frac{\sin(h\alpha)}{h})\right| \qquad (4)$$

Where h = 3, 5,7,9,11,13
V and v(t) = voltage signals
i_{TCR} = Current flowing through the reactor
I_{TCRh} = harmonic signal

But the power system installations are three phase. Using filters, these harmonics currents are cancelled [15]. If the firing angles of Th1 and Th2 are balanced, no even harmonics are generated[16].

We now consider a three phase Thyristor Controlled Reactor (TCR) as shown in fig. 4

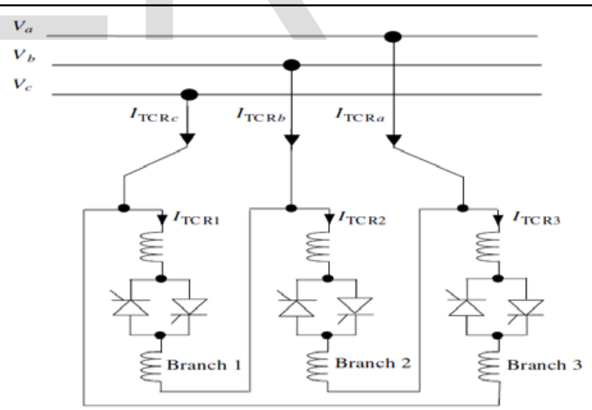

Fig. 4: Three Phase Thyristor Controlled Reactor [14]
This shows the three branches and current distribution of the three phase TCR.

We assume that harmonic components are cancelled; we now focus on the fundamental components of current.

Re-arranging equation 3, we have;

$$I_{TCRf1} = jB_{TCR}V \qquad (5)$$

Where $B_{TCR} = \dfrac{[2(\pi - \alpha) + \sin 2\alpha]}{\pi\omega L}$ = Reactor susceptances

By linear transformation technique, the three phase nodal admittances of a TCR can be obtained. Rearranging equation 5 we have:

$$\begin{vmatrix} I_{TCR1} \\ I_{TCR2} \\ I_{TCR3} \end{vmatrix} = \begin{vmatrix} -jB_{TCR1} & 0 & 0 \\ 0 & -jB_{TCR2} & 0 \\ 0 & 0 & -jB_{TCR3} \end{vmatrix} \begin{vmatrix} V_1 \\ V_2 \\ V_3 \end{vmatrix} \qquad (6)$$

The connectivity matrices for phases a, b, c:

$$\begin{vmatrix} V_1 \\ V_2 \\ V_3 \end{vmatrix} = \frac{(\pi/6)}{\sqrt{3}} \begin{vmatrix} 1 & -1 & 0 \\ 0 & 1 & -1 \\ -1 & 0 & 1 \end{vmatrix} \begin{vmatrix} V_a \\ V_b \\ V_c \end{vmatrix} \qquad (7)$$

$$\begin{vmatrix} I_{TCRa} \\ I_{TCRb} \\ I_{TCRc} \end{vmatrix} = \frac{(\pi/6)}{\sqrt{3}} \begin{vmatrix} 1 & 0 & -1 \\ -1 & 1 & 0 \\ 0 & -1 & 1 \end{vmatrix} \begin{vmatrix} I_{TCR1} \\ I_{TCR2} \\ I_{TCR3} \end{vmatrix} \qquad (8)$$

Substituting equation 7 into 6 and the result is substituted into 8, we have;
V_a, V_b and V_c are voltage in phases a, b and c respectively

$$\begin{vmatrix} I_{TCRa} \\ I_{TCRb} \\ I_{TCRc} \end{vmatrix} = \frac{1}{3} \begin{vmatrix} -j(B_{TCR1} + B_{TCR3}) & jB_{TCR1} & jB_{TCR3} \\ jB_{TCR1} & -j(B_{TCR1} + B_{TCR2}) & jB_{TCR2} \\ jB_{TCR3} & jB_{TCR2} & -j(B_{TCR2} + B_{TCR3}) \end{vmatrix} \begin{vmatrix} V_a \\ V_b \\ V_c \end{vmatrix} \qquad (9)$$

If $jB_{TCR1} = jB_{TCR2} = jB_{TCR3,}$ then 9 reduces to:

$$\begin{vmatrix} I_{TCRa} \\ I_{TCRb} \\ I_{TCRc} \end{vmatrix} = \frac{1}{3} \begin{vmatrix} -j2B_{TCR} & jB_{TCR1} & jB_{TCR3} \\ jB_{TCR1} & -j2B_{TCR} & jB_{TCR2} \\ jB_{TCR3} & jB_{TCR2} & -j2B_{TCR} \end{vmatrix} \begin{vmatrix} V_a \\ V_b \\ V_c \end{vmatrix} \qquad 10$$

Equation 10 can be represented using zero (0), positive (1) and negative sequence (2) components of a three phase system as shown in equation 11.

$$\begin{vmatrix} I_{TCR(0)} \\ I_{TCR(1)} \\ I_{TCR(2)} \end{vmatrix} = \begin{vmatrix} 0 & 0 & 0 \\ 0 & -jB_{TCR} & 0 \\ 0 & 0 & -jB_{TCR} \end{vmatrix} \begin{vmatrix} V_{(0)} \\ V_{(1)} \\ V_{(2)} \end{vmatrix} \qquad 11$$

It is deduced from equation 11 that zero sequence current does not flow into system as the reactors are connected in delta.

Using the technique above, the capacitor model can be derived as follows. For a capacitor bank, in most cases, the susceptances of the capacitors in each branch are not equal [14]. Therefore;

$$B_{C1} \neq B_{C2} \neq B_{C3} \qquad (12)$$

Where B_{C1}, B_{C2}, B_{C3} are susceptance in branches 1, 2 and 3 respectively

It follows after performing Kron's reduction on equation 9 for capacitor model we have;

$$\begin{vmatrix} I_{ca} \\ I_{cb} \\ I_{cc} \end{vmatrix} = \begin{vmatrix} -j(B_{C1} - \frac{B_{C1}^2}{\Delta B_C}) & -j\frac{B_{C2}B_{C1}}{\Delta B_C} & -j\frac{B_{C3}B_{C1}}{\Delta B_C} \\ -j\frac{B_{C1}B_{C2}}{\Delta B_C} & -j(B_{C2} - \frac{B_{C2}^2}{\Delta B_C}) & -j\frac{B_{C3}B_{C2}}{\Delta B_C} \\ -j\frac{B_{C1}B_{C3}}{\Delta B_C} & JB_{TCR2} & -j(B_{C3} - \frac{B_{C3}^2}{\Delta B_C}) \end{vmatrix} \begin{vmatrix} V_a \\ V_b \\ V_c \end{vmatrix} \qquad (13)$$

Where: $\Delta B_C = B_{C1} + B_{C2} + B_{C3,}$ $B_{C1} = \omega C_1$, $B_{C2} = \omega C_2$, $B_{C3} = \omega C3$,

But if $B_{C1} = B_{C2} = B_{C3}$, then equation 13 simplifies to equation 14 below

$$\begin{vmatrix} I_{Ca} \\ I_{Cb} \\ I_{Cc} \end{vmatrix} = \frac{1}{3} \begin{vmatrix} j2B_C & -jB_C & -jB_C \\ -jB_C & j2B_C & -jB_C \\ -jB_C & -jB_C & j2B_C \end{vmatrix} \begin{vmatrix} V_a \\ V_b \\ V_c \end{vmatrix} \qquad (14)$$

B. SVC model

A three phase model of SVC is presented in Fig. 5

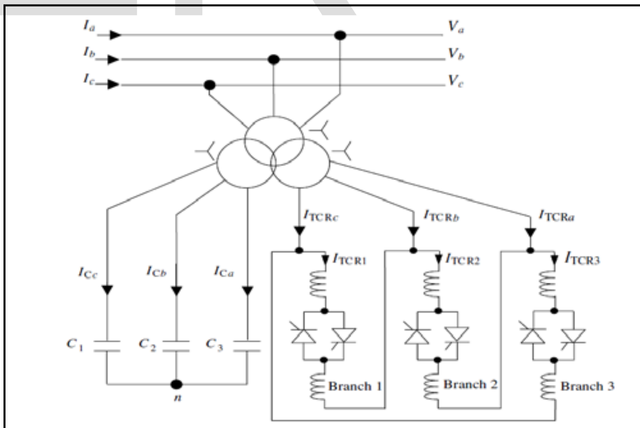

Fig. 5. Three-phase static VAR compensator [14]
This shows the interconnection and current flow of the SVC

The effective model of the SVC is derived by combining equations 10 and 14.

$$\begin{vmatrix} I_{SVCa} \\ I_{SVCb} \\ I_{SVCc} \end{vmatrix} = \begin{vmatrix} I_{TCRa} \\ I_{TCRb} \\ I_{TCRc} \end{vmatrix} + \begin{vmatrix} I_{Ca} \\ I_{Cb} \\ I_{Cc} \end{vmatrix}$$

$$= \frac{1}{3}\begin{vmatrix} j2(B_C - B_{TCR}) & -j(B_C - B_{TCR}) & -j(B_C - B_{TCR}) \\ -j(B_C - B_{TCR}) & j2(B_C - B_{TCR}) & -j(B_C - B_{TCR}) \\ -j(B_C - B_{TCR}) & -j(B_C - B_{TCR}) & j2(B_C - B_{TCR}) \end{vmatrix}\begin{vmatrix} V_a \\ V_b \\ V_c \end{vmatrix} \tag{15}$$

Equation 15 can be converted from phase co-ordinates to sequence co-ordinates by applying the matrix of symmetrical components and its inverse to equation 15 resulting to equation 16 [15].

$$\begin{vmatrix} I_{SVCa} \\ I_{SVCb} \\ I_{SVCc} \end{vmatrix} = \frac{1}{3}\begin{vmatrix} 0 & 0 & 0 \\ 0 & j(B_C - B_{TCR}) & 0 \\ 0 & 0 & j(B_C - B_{TCR}) \end{vmatrix}\begin{vmatrix} V_{(0)} \\ V_{(1)} \\ V_{(2)} \end{vmatrix} \tag{16}$$

It can be deduced from equation 16 that zero sequence current does not flow into system as the star point of the capacitors are floating.

$$I_{SVC(1)} = jB_{SVC}V_{(1)} \tag{17}$$

Where:

$$B_{SVC} = B_C - B_{TCR} = \frac{1}{X_C X_L}\left(X_L - \frac{X_C}{\pi}[2(\pi - \alpha) + \sin 2\alpha]\right)$$

$$X_L = \omega L, X_C = \frac{1}{\omega C} \tag{18}$$

B_{SVC} - susceptance of the SVC
X_L - Inductive reactance, X_C – Capacitive reactance
ω – angular frequency

3.2SVC Control Module

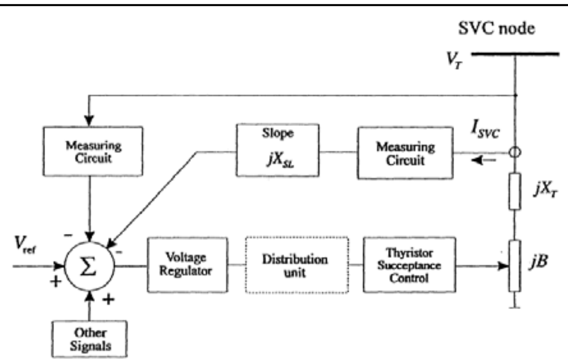

Fig. 6. Basic SVC Model [15]
This shows the different module of the SVC.

The SVC Control comprises of following elements [16]:

- The voltage and current measuring (and filtering) circuit.
- A regulator including possible additional signals fed to the reference point.
- Additional control signals are used for system damping improvement.
- A distribution unit.
- A model of the Thyristor susceptance control module.
- A model of the interface with the power system

A. Measuring Module

The measuring module for current and voltage will be represented by approximated Transfer function as [16]:

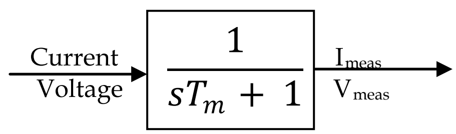

Hence transfer function of measuring module, M(s) is given as:

$$M(s) = \frac{1}{sT_m + 1} \tag{19}$$

Where: T_m is measuring circuit time constant

B. Voltage Regulator Module

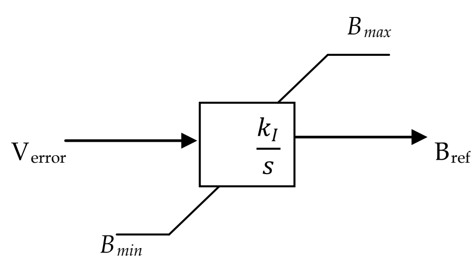

Hence transfer function of measuring module, R(s) is given as:

$$R(s) = \frac{K_I}{s} \tag{20}$$

Where K_I is integrator gain

C. Thyristor susceptance control model

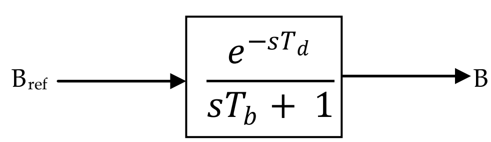

Hence transfer function of measuring module, T(s) is given as:

$$T(s) = \frac{e^{-sT_d}}{sT_b + 1} \quad (21)$$

Where: gating delay (dead time) T_d is neglected as it is very small (≈ 1/12 th cycle of the fundamental), [16]

T_b is the effect of Thyristor firing sequence control.

$$V_T = V_{ref} + I_{SVC} X_{SL} \quad (22)$$

V_T- Output voltage, V_{ref}- reference voltage, I_{SVC} – SVC current, Slope reactance

D. **Distribution Unit**

This module determines the number of stages of capacitor bank and/or reactor required for reactive power compensation.

3.3 Modeling of Discrete- Time PID Controller

The PID controller has a transfer function as given below [17] :

$$G_c(s) = K_p + \frac{K_I}{s} + K_D(s) \quad (23)$$

In time domain, equation 23 becomes:

$$U(t) = K_p e(t) + K_I \int_0^t e(t)dt + K_D e_f(t) \quad (24)$$

Where: K_I = Integral gain and K_D = Derivative gain
Where: u - controller output (controlled variable),
e - The control error.

$$e(t) = r(t) - y(t) \quad (25)$$

Where: r is the reference or set point, y is the process measurement, e_f is the filtered control error. It is the output of the following low-pass filter:

$$e_f(s) = \frac{1}{T_f s + 1} e(s) \quad (25a)$$

Where: T_f is filter time constant
$T_f = aT_D$, a is typically 0.1

Differentiating equation 24 and solving for $U_{(tk)}$ gives the Discrete – Time PID Controller,

$$U_{(tk)} = U_{(tk\text{-}1)} + K_p[e_{(tk)} - e_{(tk\text{-}1)}] + \frac{K_{ph}}{T_I} e_{(tk)} + \frac{K_p T_D}{h}[e_{f(tk)} - 2e_{f(tk\text{-}1)} + e_{f(tk\text{-}2)}] \quad (26)$$

4 System Integration

Having derived models for the various components, the models are integrated. Putting equations 17, 19, 20, 21, 22, into block, the simplified SVC block is derived as presented in fig. 7.

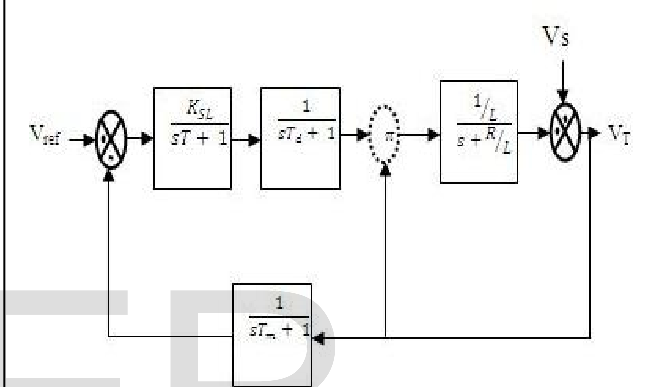

Fig. 6. Basic SVC Model [15]
It shows the different modules and transfer functions derived for the SVC. They are integrated together from which the overall system transfer function is derived.

From fig. 7, the overall system transfer function is derived easily as follows:

$$\Delta V_T(s) = \left|\frac{R(s)T(s)D(s)}{1 + R(s)T(s)D(s)M(s)}\right| \Delta V_{ref}(s) + \left|\frac{1}{1 + R(s)T(s)D(s)M(s}\right| \Delta V(s) \quad (27)$$

Transfer function of SVC control system when the SVC is either generating or absorbing reactive power is given in equation 28 below.

$$\frac{\Delta V_T}{\Delta V_{ref}} = \frac{R(s)T(s)D(s)}{1 + R(s)T(s)D(s)M(s)} \quad (28)$$

Where: $M(s) = \frac{1}{sT_m + 1}$, $T(s) = \frac{1}{sT_d + 1}$, $D(s) = \frac{1/L}{s + R/L}$,

$$R(s) = \frac{K_{SL}}{sT + 1}$$

The response of the system when the SVC is neither generating nor absorbing reactive power is determined from equation 29. At this point, $V_{ref} = 0$

$$\frac{\Delta V_T(s)}{\Delta V_S(s)} = \frac{1}{1 + R(s)T(s)D(s)M(s)} \quad (29)$$

Substituting Standard SVC data into equation 28 results in the transfer function given below:

$$G(s) = \frac{\Delta V_T(s)}{\Delta V_S(s)} = \frac{0.3s^2 + 0.1s + 0.02}{1.42s^2 + 0.05s + 0.03} \quad (30)$$

5 Result and Discussion

The performance of the system represented by equation 30 is tested using Matlab tool and the response is as presented in fig.8:

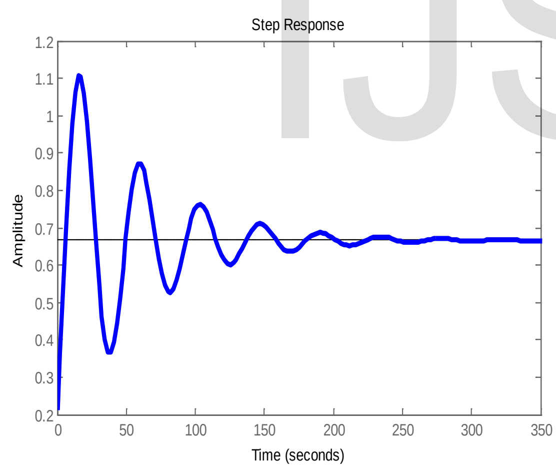

Fig. 8: System Response without PID controller
It is the basics for the analysis of the design. Overshoots, settling time, rise time are obtained from it.

The performance of the system is determined using Matlab tool as follows:

Rise Time: 4.8322s
Settling Time: 235.9588s
Overshoot: 65.9052%
Undershoot: 0
From the response presented fig. 8 and system performance stated above, it can be deduced that the operation of the system is prone to vibration. The settling time for response is very high resulting to increased inaccuracy and possible instability. The percentage overshoot also shows the system precision can be improved. Hence, PID is introduced to further enhance the performance of the SVC technique.
The performance of the system with the addition of PID controller shows an improved and optimized system as presented in fig. 9.

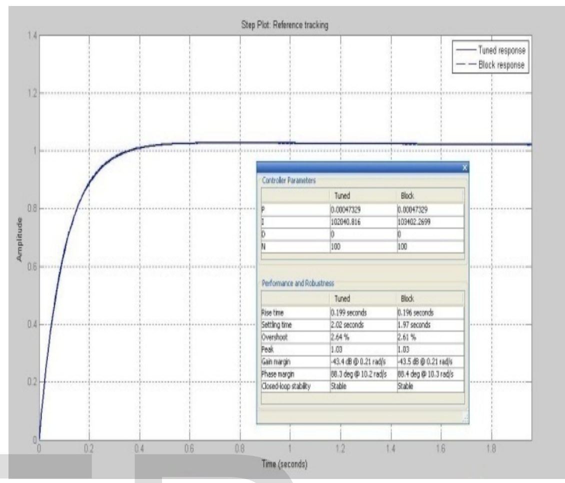

Fig. 9. System Response with PID controller
It is the basics for the analysis of the design. Overshoots, settling time, rise time are obtained from it.

The following parameters were obtained after the addition of a PID controller to the control system:
Rise time = 0.199s
Settling time = 2.20s
Overshoot = 2.64%
Peak = 1.03

The controller has been used to optimize the compensation process of reactive power given faster, more accurate and stable response. The controller is tunes automatically following a disturbance. At the instant of tuning, the PID controller has the following gain:

$$K_P = 0.00047329$$
$$K_i = 102040.816$$
$$K_d = 0$$
$$N = 100 \quad (31)$$

The controller transfer function when connected in parallel form is given as:

$$G_C(s) = K_P + \frac{K_I}{s} + D\frac{N}{1 + N/S} \quad (32)$$

Substituting equation 31 into equation 32, gives:

TABLE 1

TYPICAL PARAMETERS FOR SVC MODEL [15]

Module	Parameter	Definition	Value
Measuring	Tm	Measuring circuit time constant	0.001 - 0.005s
Thyristor Control	Td Tb	Gating transport delay Thyristor firing sequence control delay	0.001s 0.003 - 0.006s
Voltage Regulator	Ki	Integrator gain	Adjustable
Slope	XSL	Steady state characteristic slope	0.01 - 0.05pu.
Time constant	T	Time constant	0.002 - 0.005s
	KSL	$K_{SL} = \frac{1}{X_{sl}}$	
Network	Z	Impedance	(0.072+j0.12)Ω
Module	Parameter	Definition	Value
Measuring	Tm	Measuring circuit time constant	0.001 - 0.005s
Thyristor Control	Td Tb	Gating transport delay Thyristor firing sequence control delay	0.001s 0.003 - 0.006s
Voltage Regulator	Ki	Integrator gain	Adjustable
Slope	XSL	Steady state characteristic slope	0.01 - 0.05pu.
Time constant	T	Time constant	0.002 - 0.005s
	KSL	$K_{SL} = \frac{1}{X_{sl}}$	
Network	Z	Impedance	(0.072+j0.12)Ω
Module	Parameter	Definition	Value
Measuring	Tm	Measuring circuit time constant	0.001 - 0.005s
Thyristor Control	Td Tb	Gating transport delay Thyristor firing sequence control delay	0.001s 0.003 - 0.006s

$$G_C = 0.00047329 + \frac{102040.816}{s} \tag{33}$$

Table1 shows standard SVC parameters substituted into the corresponding equations to derive a dynamic equation representing the performance of the design

The closed loop transfer function consists of the transfer functions of the controller and SVC.

$$G(s) = \frac{0.0001419s^3 + 1.21s^2 + 4041s + 808.3}{1.42s^3 + 1.212s^2 + 4041s + 808.3} \tag{34}$$

It is very important for the entire to maintain its stability after the connection of the controller. The operation of the controller should not create disturbance or make the network unstable. Hence, the stability of the controller with the SVC is tested using Nyquist stability criterion as presented below. Equation 34 was tested using Matlab tool for stability. The stability of the system is presented in fig. 10.

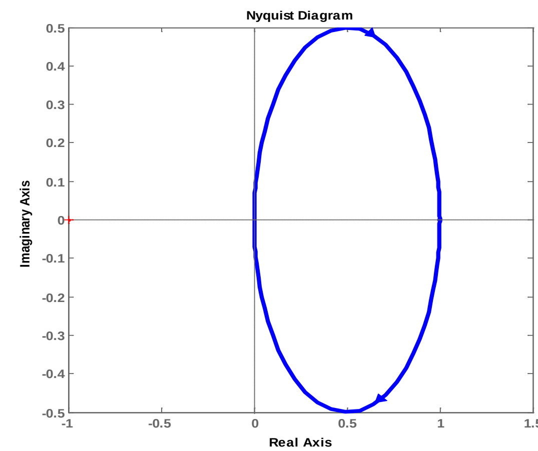

Fig. 10.Nyquist plot showing system stability

It is used for stability analysis of the design

All the roots of the dynamic equation must lie on the left-hand side of the s-plane for it to be stable. Equation 34 has no positive root indicating that all the roots lie on the left-hand side of the s-plane.

In [17],Nyquist stability criterion was presented as follows: "A feedback system is stable if and only if the contour ,TL in the JL(s)-plane does not encircle the (-1, 0) point when the number of poles of L(s) in the right -hand s-plane is zero (P = 0)".

The Nyquist plot presented in fig. 10 shows that the contour does not encircle (-1, 0) point and equation 34 has no positive root indicating that all the roots lie on the left -hand side of the s-plane. Therefore, the design presented in this paper is stable.

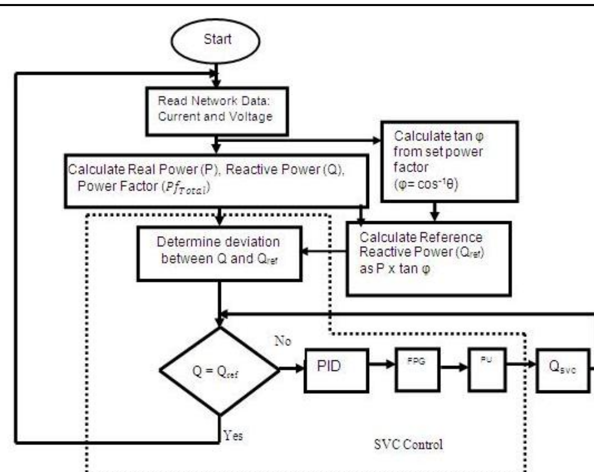

Fig. 11. Control System Algorithm

Control system Algorithm is presented in fig. 11. The control law is the difference between measured reactive power and a set value determined from a reference power factor. Upon a deviation between reference and set values, the PID tunes automatically to determine new controller gains, firing angle of thyristor and required compensation to return and maintain measured value to be equal to set value

6 Conclusion

The simulation results show a good improvement in the transient response of the control loop. The gain of the controller is tuned automatically following a change in network dynamics to balance and maintain stability. The percentage overshoot shows an improvement on compensation accuracy. The results show that the controller is efficient and easy to implement.

Reference

1. Ganesh, K. V. (2010). An Adaptive Control Strategy for DSTATCOM Applications in an Electric Ship Power System, IEEE TRANSACTIONS ON POWER ELECTRONICS, VOL. 25, NO. 1,
2. Amstrom, K. J., &Wittenmark, B. (1995). Adaptive control (2nd edition). Addison-Wesley 1995, ISBN 0-201-55866-1
3. Bishnu, P. M., Eswar, S. R., &Vithal, J.V.R., (2006). SVPWM Switched DSTATCOM for Power Factor and Voltage Sag Compensation —International conference on Power Electronics, Drives and Energy Systems, IEEE, pp. 1-6.
4. Szabó, D. (2014) Control of a SVC for power factor correction, Educational grant agency (KEGA) Nr: 030ŽU-4/2014
5. Zoran, V. (2000). A Tutorial on adaptive control: The self tuning approach, Dept. of control and computer engineering in automation, Faculty of Electrical Engineering and Computing, University of Zagrab, Croatia.
6. Lavretsky, E. (2002). Adaptive Control: Introduction, Overview, and Applications - Robust and Adaptive Control Workshop, IEEE workshop slides
7. Amstrom, K. J., &Wittenmark, B. (1995). Adaptive control (2nd edition). Addison-Wesley 1995, ISBN 0-201-55866-1
8. Nokian Capacitors. (2010). High Voltage Reactive Power Compensation and Harmonic Filtering Products Guide: Alstom Grid Worldwide Contact Centre, UK.
9. Gupta, J.B. (2005). A course in Power system (10th Edition) pp293-296" Katson Books, New Delhi, India.
10. Sandesh et al, (2012), Improve Power Factor and Reduce the Harmonics Distortion of the System, Department of Electrical Engineering, Samrat Ashok Technological Institute Vidisha, MP, INDIA, Research Journal of Engineering Sciences with reference" Vol. 1(5), 31-36, Res. J. Engineering Sci. ISSN 2278 – 9472"
11. Moran et al, (1995), A three phase active power filter operating with fixed switching frequency for reactive power and current harmonic compensation, IEEE Transactions on Industrial Electronics, Vol.42, No. 4
12. Kumar et al, (2013), Simulation & Design of Power Factor Correction Prototype for BLDC Motor Control, European Scientific Journal, vol.9, No.12 ISSN: 1857 – 7881 (Print) e - ISSN 1857- 7431.
13. ABB Product manual (2000). SVC – An Insurance for improve grid system stability and reliability, ABB AB FACTS, Sweden
14. Acha, E., Esquivel, C.R.F., Perez, H. A., & Camacho, C.A. (2004). FACTS modeling and simulation in power system Networks. (Chap 2, pp. 34-36): John Wiley & Sons Ltd, British Library
15. ABB Power Systems (1996). Modeling of SVC for Power System Studies, Information NR 500 -026E, AB-S-721 64 Vasteras, Sweden
16. Boudjella, H., Gherbi F. Z., &Lakdja, F. (2008). Modeling and Simulation of Static Var Compensator (SVC) in Power System Studies by Matlab. The annals of "Dunarea De Jos" University of Galati Fascicle iii, vol.31, no.1, issn 1221-454x Electrotechnics, electronics, automatic control, informatics.
17. Dorf, R.C., & Bishop, R. H. (2011). Modern Control System, (12th Edition), Pearson Education, Inc., Upper Saddle River, New Jersey 07458, USA

BIOGRAPHIES

Dr. Gordon Ononiwu - Received his B.Eng, in Electrical and Electronic Engineering from the Federal University of Technology (FUTO), Owerri, his M.Sc in Computer Systems Engineering. From Halmstad University in Sweden, and his PhD in Computer Engineering from FUTO. He is a senior Lecturer at the department of Electrical and Electronic Engineering of the Federal University of Technology, Owerri. He is a fellow of the

ISSN 2229-5518

Swedish Institute (SI), and also an International Faculty Fellow (2015/2016) at the Massachusetts Institute of Technology (MIT). He was a guest scholar at the Centre for Research on Embedded Systems (CERES) in Sweden (2009 - 2011). He is a member of Nigerian Society of Engineers and is registered with COREN. His research interest is in the field of embedded systems engineering.
Email: gordon.ononiwu@yahoo.com

Onwumere Justine Chimezie - Received his B.Eng, in Electrical and Electronic Engineering from Nnamdi Azikiwe University, Awka, Nigeria. He is currently pursuing the M.Eng degree in Electrical and Electrionic Engineering from Federal University of Technology, Owerri, Nigeria. His research interests include: Control System Design, Aircraft Control System Design, and Power System Automation. Email: just2cherish44@gmail.com

Dr. James Onojo- Received his B.Eng, in Electrical and Electronic Engineering from the Federal University of Agriculture, Makurdi, his M.Sc & Ph.D in and Electronic Engineering of the echnology, Owerri. His research f Power systems engineering and ns.
Email: jamesonojo@yahoo.com

Ezema Longinus- Received his B.Eng. degree in Electrical Electronic Engineering from Nnamdi Azikiwe University, Nigeria in 2004 and the M.Sc. in Telecommunication System from Blekinge Institute of Technology, Sweden in 2007. He is currently pursuing the Ph.D degree in Electronic Engineering from University of Nigeria Nsukka, Enugu State, Nigeria. He is currently a lecturer at Federal University of Technology Owerri. His research interests include wireless mobile communication and mobile location systems. He is a member of Nigerian Society of Engineers (NSE) and Council for the Regulation of Engineering in Nigeria (COREN).
Email: ezemms@yahoo.com

Power Systems Engineering from the Federal University of Technology, Owerri (FUTO). He is a senior Lecturer at the